PROFESSOR JING GUO (Orcid ID : 0000-0003-0278-0808)

PROFESSOR HONG WANG (Orcid ID : 0000-0003-3991-6203)

Article type : Article

Heterogeneous Multilayer Dielectric Ceramics Enabled by Ultralow Temperature Self-Constrained Sintering

Jianyu Hao,[1] Fang-Zhou Yao,*[1] Qibin Yuan,[1] Xinwei Xu,[1] Bin Yao,[1] Jiufeng Dong,[1]
Jing Guo,[1] Hong Wang*[1,2]

[1] State Key Laboratory for Mechanical Behavior of Materials & School of Electronic and Information Engineering, Xi'an Jiaotong University, Xi'an 710049, China.

[2] Department of Materials Science and Engineering & Shenzhen Engineering Research Center for Novel Electronic Information Materials and Devices, Southern University of Science and Technology, Shenzhen 518055, China.

* Corresponding author: yaofangzhou@mail.xjtu.edu.cn (Fang-Zhou Yao);
wangh6@sustech.edu.cn (Hong Wang)

Abstract

In the present work, heterogeneous multilayer ceramics based on two representative dielectrics, low-K Li_2MoO_4 (LM) and high-K $[(Li_{0.5}Bi_{0.5})_xBi_{1-x}][Mo_xV_{1-x}]O_4$ (LBMV), are successfully acquired using a convenient approach of self-constrained sintering at an ultralow temperature of 600 °C. These two materials with proximate but distinct sintering temperature ranges mutually act as constrained layers to each other in the process of densification, yielding significantly suppressed in-plane shrinkage of the LM/LBMV heterogeneous multilayer ceramics. Moreover, the dense heterostructures are endowed with decent mechanical and microwave dielectric properties. This work offers a new paradigm for facilely integrating heterogeneous dielectric materials for ULTCC (ultralow temperature co-fired ceramics) applications.

Keywords: Microwave dielectric materials, Heterogeneous multilayer ceramics, ULTCC technology, Self-constrained sintering

1. Introduction

Microwave dielectric ceramics are ubiquitous in modern information or communication industries, such as the satellite communication systems, mobile handheld devices, and avionics including civil and military radar systems, etc., since they are indispensable ingredients for the key electronic components of resistors, capacitors, and inductors, etc.[1-9] To meet the increasing demand for high performance multifunctional communication systems with minimized volume and light weight, integration of various passive components through a low temperature co-fired ceramic (LTCC) technology has attracted tremendous attentions from both the academic and industrial players.[10-12] However, the potential issues of mismatched shrinkage, delamination, warpage, and undesired intermediate phase in the dielectric heterostructures post enormous challenges for the miniaturization of microwave devices via a facile LTCC approach.[13-17] To resolve them, four strategies are generally adopted, namely, adding glass phase, constrained sintering, cold sintering, and self-constrained sintering. The first one is mainly achieved through adding glass phase to the heterogeneous materials to tune their physical and chemical properties to be compatible. Korea Institute of Science and Technology and Murata Manufacturing have successfully applied this method to co-fire certain heterostructures, such as Al_2O_3/($ZnNb_2O_6$-TiO_2), Mg_2SiO_4/$BaTi_4O_9$, Mg_2SiO_4/$BaNb_2Ti_4O_{12}$($Nd_2Ti_2O_7$) and so on.[16-19] However, addition of glass phase would inevitably sacrifice a great portion of electrical properties of the heterostructures, which limits the application of this method to certain microwave dielectrics. The second one is applying a uniaxial pressure to the rigid substrates attached to the top and bottom surfaces of the heterogeneous samples to inhibit the in-plane shrinkage during sintering process.[20-23] Unfortunately, applying external pressure and additional machining procedures including addition and removal of rigid substrates significantly increase the processing costs, rendering this approach disadvantageous for mass production. The third approach of cold sintering makes the sample to reach a densified state by a dissolution-precipitation process, and now it has been employed in various materials, such as MLCC,[24,25] microwave dielectric devices,[26,27] thermoelectric materials,[28] solid electrolytes,[29] etc. However, the requirement of enormous external pressure is a major disadvantage for practical implements of this method. The recently developed self-constrained sintering takes advantage of the appropriate but distinct densification temperature ranges of two microwave dielectric materials, which densify and constrain mutually during sintering to form a multilayer heterostructure with alternatively laminated lower-temperature sintering layers and higher-temperature sintering layers.[30-33] Compared with the above three maneuvers, self-constrained sintering without compromising the microwave dielectric properties and needing no additional processing seems more promising. Up to now, only certain efforts have been devoted to developing glass-ceramic/glass or glass/alumina laminates using self-constrained sintering, leaving plenty of room for developing high-end multifunctional ceramic/ceramic heterostructures for LTCC applications based on this sintering method.

In this work, heterogeneous multilayer ceramics based on two representative ULTCC microwave dielectric materials, low-K Li_2MoO_4 (LM) and high-K $[(Li_{0.5}Bi_{0.5})_xBi_{1-x}][Mo_xV_{1-x}]O_4(x=0.098)$ (LBMV) (more details shown in **Table 1**), were prepared by the self-constrained sintering technique.[34,35] When heated at a relatively low temperature, the high-K non-shrinking LBMV with a higher sintering temperature acts as a constrained layer to the low-K LM with a lower sintering temperature, and their roles reverse at a relatively high temperature, yielding significantly suppressed in-plane shrinkage in the LM/LBMV heterogeneous multilayer ceramics. Moreover, the heterostructures sintered at an ultralow temperature of 600 °C are endowed with decent mechanical and microwave dielectric properties, demonstrating the great potential of self-constrained sintering for ULTCC applications.

2. Experimental

Preparation of LM and LBMV Ceramics. The LM and LBMV ceramics were prepared by a conventional solid-state reaction route. Raw materials Li_2CO_3 (>98%, Sino pharm Chemical Reagent, Shanghai, China), MoO_3 (>99.5%, Yu tong Chemical Reagents, Tianjin, China), Bi_2O_3 (>99%, Sino pharm Chemical Reagent, Shanghai, China) and V_2O_5 (> 99.6%, Macklin Chemical Reagent, Shanghai, China) were weighed according to the stoichiometry of Li_2MoO_4 and $[(Li_{0.5}Bi_{0.5})_xBi_{1-x}][Mo_xV_{1-x}]O_4$ (x=0.098). The weighed powders were ball milled in alcohol for 4 h using a planetary mill (Nanjing Machine Factory, Nanjing, China). After drying, these powders were then calcined at 500-600 °C for 4 h at ambient condition. Then the calcined powders were re-milled again for 4 h and pressed into cylinders (10 mm in diameter and 4-5 mm in height) at 200 MPa. The green pellets were sintered at 500-680 °C for 2 h.

Preparation of LM/LBMV heterogeneous multilayer Ceramics. The LM/LBMV heterogeneous multilayer ceramics were fabricated by following the tape-casting and lamination procedures, as sketched in **Figure 1**, which mainly consist of four steps, i.e., tape-casting, cutting, lamination and densification. Prior to those, LM and LBMV slurries were prepared. The as-received LM and LBMV powders from the aforementioned process were mixed with a solution of ethyl alcohol, methyl ethyl ketone and glycerol trioleate as the dispersant for 8 h to form the uniform slurries. Then the slurries were subjected to another ball-milling for 8 h, while adding polyvinyl butyral (PVB) as the binder and polyethylene glycol (200) (PEG200) and dibutyl phthalate (DBP) as the plasticizer. Afterward, the LM and

LBMV slurries were successively cast to form a monolayered LM/LBMV green sheet with a thickness of 40-50 μm. The green sheets were cut and laminated to form cylindrical pellets (10 mm in diameter and 5 mm in thickness) under 30 MPa at 70 °C for 20 min, followed by a cold isostatic pressing at 200 MPa for 5 min. Finally, the laminated samples were heated at 350 °C for 12 h with a slow heating rate of 0.2 °C/min to remove all the organic additives. And then, the multilayered LM/LBMV samples were treated at 540 °C for 1 h and 600 °C for 2 h successively with a heating rate of 3 °C/min.

Characterizations. The phase structures of the LM and LBMV powders were investigated using X-ray diffraction (XRD) with Cu-Kα radiation (SHIMADZU XRD-7000, Tokyo, Japan). The cross sectional microstructures of the samples were examined by a scanning electron microscope (SEM, Quanta F250, FEI, USA). Nano measure software was used to analyze the grain size distribution of LM and LBMV ceramics sintered at different temperatures. Vickers Hardness (H_v) was obtained by the indentation technique on polished ceramic surfaces with a nanoindenter and a mechanical load of 0.098 N at room temperature. H_v can be expressed by the formula: $H_v = 0.0018544\ (P/d^2)$, where P is the applied force, and d is the average diagonal length of the indentation pyramid. The sintering temperature dependent shrinkage of samples was collected using a vernier caliper. Microwave dielectric properties were measured using the $TE_{01\delta}$ shielded cavity method with a network analyzer (8720ES, Agilent, Palo Alto, CA) and a thermal chamber. The temperature coefficient of resonant frequency TCF (τ_f) of the samples can be calculated by the following formula:

$$\mathrm{TCF} = (f_{85}-f_{25})/\ (f_{25}\times 60)\times 10^6\ (\mathrm{ppm/°C}) \qquad \textbf{(1)}$$

Where f_{85} and f_{25} are the $TE_{01\delta}$ resonant frequencies at 85 °C and 25 °C, respectively.

3. Results and discussion

Figure 2a presents the XRD patterns of the LM and LBMV ceramics sintered at their optimal temperatures. For LM, all the diffraction peaks matched well with those of the standard samples (JCPD card No. 12-0763), and no secondary phase was observed, indicating the perfect crystallization of the as-sintered LM ceramics. As a solid solution between $BiVO_4$ and $(Li_{0.5}Bi_{0.5})MoO_4$, the crystal structure of LBMV gradually evolves from a tetragonal scheelite structure of $BiVO_4$ to a monoclinic structure of $(Li_{0.5}Bi_{0.5})MoO_4$ with increasing the content of $(Li_{0.5}Bi_{0.5})MoO_4$ (around 10mol%).[35,36] It can be observed from **Figure 2a** that the as-received LBMV polycrystals exhibit the identical tetragonal scheelite structure with pristine $BiVO_4$ ceramics, evidenced by the presence of characteristic peaks of (011) and (020) for tetragonal scheelite structure, as shown in **Figure 2b and c**, respectively. It suggests that $(Li_{0.5}Bi_{0.5})MoO_4$ and $BiVO_4$ have formed a solid solution with a tetragonal scheelite structure as $BiVO_4$, and the LBMV powders have been successfully prepared.

Generally, for ceramic sintering, pinning down the optimized sintering temperature is crucial and any deviation from the optimal heat treatment temperature will result in the variation of microstructure and negatively affect the properties of ceramics. However, for self-constrained sintering derived heterogeneous multilayer ceramics, a wide sintering temperature range overweighs an optimal sintering temperature of specific material of choice for practical implements. Therefore, the sintering temperature dependence of average grain size and microwave dielectric properties of LM and LBMV were investigated, as shown in

Figure 2d and **Figures S1-3**. It can be found that LBMV materials possess a wide sintering temperature window from 550 °C to 680 °C, within which the grain size slightly changes (refer to **Figure 2d** and **Figure S2**) and the decent microwave dielectric properties have been obtained (**Figure S3**). The sintering temperature window for LM ceramics is relatively narrow, hence their grain size grows sharply (**Figure 2d** and **Figure S1**) and their microwave dielectric properties get deteriorated (**Figure S3**) when the sintering temperature goes beyond the optimal sintering temperature around 540 °C. Despite that, LM ceramics fired at high temperatures can still deliver satisfying microwave dielectric properties. Accordingly, to obtain high performance LM/LBMV heterogeneous multilayer ceramics using the self-constrained sintering approach, the sintering temperature of LBMV should be compromised marginally to reach the optimal sintering range of LM.

To unveil the sintering behavior of LM/LBMV heterogeneous multilayer ceramics, the evolution of their microstructure with sintering temperature within the range from 500 to 600 °C was studied, as displayed in **Figure 2e**. The LM layers gradually get densified with the temperature going up to 540 °C. Beyond this point, the grain size of LM phase grows dramatically, whereas no distinguished change of grain size can be observed in the LBMV counterparts. In the meantime, LBMV layer acts as a rigid substrate for LM to suppress its in-plane shrinkage during the densification process. The LM sandwiched between rigid LBMV layers is subjected to in-plane stress merely, and the stresses applied to both surfaces of LM layers are identical. Therefore, the absence of out-plane component of stress prevents the occurrence of warpage, delamination, or crack in the multilayers. When the temperature rises to around 600 °C, LM phase has come to fully densification and LBMV also begins its densifying procedure, although the change of grain size in LBMV is inconspicuous. At this stage, the rigid LM layer plays a reversed role as the constrained layer to the LBMV for the same purpose as aforementioned.

To verify the quality of self-constrained sintered LM/LBMV heterogeneous multilayer ceramics, in-depth studies were conducted to preclude the existence of undesired flaws, such as warpage, delamination, intermediate phases, etc., which are detrimental to the properties of these materials. **Figure 3a** provides the photograph of as-prepared LM/LBMV heterogeneous multilayer ceramics, where no warpage or fracture is observable. Further cross-sectional microstructure studies reveal that the profile of each individual layer of the sample is distinct, and no delamination is found, despite some minor pores are inevitably traced, particularly in the LM layers (see **Figures 3b-d**). The EDX elemental analyses are shown in **Figures 3e-j**. The sharp contrast tells that the elements Mo and V mainly reside in the LM and LBMV layers, respectively, and no element migration or secondary phase occurs at the interfaces, implying no side reaction between the two active layers. It should be noted that the emergence of element Bi in LM is mainly ascribed to the overlapped energy spectra of Mo and Bi elements (refer to **Figure S4**).

For the practical applications of heterogeneous multilayer ceramics, not only the microstructure mentioned above but also the mechanical properties of individual layers and the interfaces are of paramount importance. Hardness characterizes the material's local resistance to external force and strain. It is closely related with the material's elastic stiffness, strength, toughness and so on. For ceramics, density has a direct bearing on the hardness. Herein, the hardness of LM and LBMV individual polycrystals and LM/LBMV heterogeneous multilayer ceramics were collected, as illustrated in **Figure 4a** and **Figure S5**. Both LM and LBMV pristine ceramics sintered at 600 °C have a lower hardness than those sintered at the optimal temperatures of 540 °C and 650 °C, respectively, due to the lower density induced by the deviation from the optimal sintering temperature. It is interesting to note that the LM/LBMV heterogeneous multilayer ceramics have slightly superior hardness than those of LM and LBMV individual samples sintered at the same temperature of 600 °C. And more importantly, the interface region of the LM/LBMV heterostructures is endowed with a surprisingly high hardness, sandwiched by the values for the LM and LBMV individual phases, demonstrating the feasibility of using self-constrained sintering approach to realize solid bonding between heterogeneous materials.

As demonstrated above, self-constrained sintering is a feasible approach to co-fire LM/LBMV heterogeneous multilayer ceramics. And beyond that, self-constrained sintering has the merit of restraining the in-plane shrinkage effectively. It is of great importance to accurately control the in-plane shrinkage of LTCC tapes to guarantee the reliability of final LTCC devices with high integration, considering the relatively large in-plane shrinkage ranging from 12% to 16% of LTCC tapes after normal sintering. The in-plane and out-plane shrinkages of LM and LBMV ceramics, and LM/LBMV heterogeneous multilayer ceramics during co-firing have been also studied, as plotted in **Figures 4b and c**, respectively. For pure LM and LBMV samples prepared by the same tape casting method, the isotropic shrinkage is observed, namely, nearly equal shrinkage along the in-plane and out-plane directions within the range from 12% to 17% at the final sintering stage (see **Figure 4b**). However, in the case of LM/LBMV heterogeneous multilayer ceramics, a different scenario from those of LM and

LBMV emerges. It is intriguing to note that the LM/LBMV heterostructures present anisotropic shrinkage during sintering process. More specifically, the out-plane shrinkage far exceeds the in-plane one (~24% *vs* 10%, refer to **Figure 4c**), or the in-plane shrinkage of the heterogeneous multilayer ceramics is greatly suppressed by the self-constrained sintering, which is beneficial for practical implements. In order to elaborate the shrinkage process, a parameter of out-plane/in-plane shrinkage ratio, i.e., the out-plane shrinkage divided by the in-plane shrinkage, is introduced. **Figure 4d** provides the temperature-dependent out-plane/in-plane shrinkage ratios of LM and LBMV ceramics, and LM/LBMV heterogeneous multilayer ceramics. It is found that the shrinkage ratios of LM and LBMV ceramics both approach one unit in the sintering temperature range, further confirming the isotropic shrinkage in these two pristine materials, which are free of external strain during the densification process. However, the corresponding value of LM/LBMV heterostructures varies between 2.2 to 3.0, mainly attributed to the variant shrinkage mechanisms at different temperature ranges. At the first sintering stage (approximately lower than 540 °C), the LM layers gradually get densified, yet the LBMV layers nearly remain unchanged. Thus, the LBMV layer acts as a rigid substrate, which exerts a tangential force on LM to suppress its in-plane shrinkage during the densification process; while the out-plane shrinkage of LM is almost unconstrained, resembling to the model ***a*** sketched in **Figure 4d**. Thus, the shrinkage ratio of LM/LBMV heterogeneous multilayer ceramics is large at this stage. As the temperature rises, the LBMV layers begin to densify around 540 °C, and LM still has marginal shrinkage, which can be confirmed by LM and LMBV shrinkage curves in **Figure 4b** and microstructure evolution in **Figure 2e**. The tangential force between LM and LBMV phases decreases, and no external force is applied along the out-plane direction, resulting in reduced shrinkage ratio of LM/LBMV heterostructures (corresponding to model ***b***). Finally, when the temperature is higher than 560 °C, LM has become fully densified, and it can serve as a constrained layer to the LBMV. At this time, the LM layer would exert an in-plane tangential force on LBMV to suppress its in-plane shrinkage, while LBMV is nearly free of strain along the out-plane direction (see model ***c***). Thus, the shrinkage ratio of LM/LBMV heterostructures slightly rises above 560 °C. Overall, LM/LBMV heterogeneous multilayer ceramics prepared by self-constrained sintering show significantly restrained in-plane shrinkage.

Microwave dielectric properties of LM and LBMV ceramics and LM/LBMV heterogeneous multilayer ceramics sintered at 600 °C are presented in **Figure 5a**. It can be found that both LM and LBMV pristine ceramics possess fine microwave dielectric properties. The as-received LM polycrystals bear a permittivity of 4.9, a Q×f value of 18000 GHz, and a TCF value of -180 at a frequency of 12.3 GHz, despite the properties are slightly compromised as they were not sintered at the optimal temperature (540 °C), which could yield an optimal permittivity of 5.5, a Q×f value of 43000 GHz, and a TCF value of -160 at a frequency of 12.0 GHz (refer to **Figure S3**). This is mainly ascribed to the narrow sintering temperature window of LM materials. When the sintering temperature is higher than the optimal temperature, abnormal grain growth occurs (see **Figure S1**), which leads to decreased density and deteriorated microwave dielectric properties. In the case of LBMV ceramics sintered at 600 °C, a permittivity of 73, a Q×f value of 6600 GHz, and a TCF value of +19 at a frequency of 4.0 GHz can be obtained. And these parameters are comparable to those of LBMV heated at the optimal temperature of 650 °C (permittivity ε_r: 81, Q×f: 8000 GHz, TCF: +10 at a frequency of 4.2 GHz, see **Figure S3**), benefiting from the wide sintering temperature range of LBMV. Both LM and LBMV polycrystals sintered at 600 °C are qualified for practical applications. And fortunately, the LM/LBMV heterogeneous multilayer ceramics prepared at 600 °C by the self-constrained sintering are also endued with decent microwave dielectric properties with a permittivity of 9.5, a Q×f value of 15300 GHz, and a TCF value of 13.4 at a frequency of 9.1 GHz. Generally, the properties of composite materials are predictable and can be determined by the individual properties, the volume fractions and the spatial distribution of each component. It is known that dielectric permittivity is an important parameter for the microwave dielectric materials and many models have been proposed to predict the average permittivity of two-phase composites. For instance, for the 2-2 type composite materials, i.e., a diphasic composite with self-connectivity of 2 dimensions connecting with each other, there are two known models to predict the average permittivity. One is that the composite materials are aligned parallel to the electric field (Equation (2)), the other is that the composite materials are aligned perpendicular (series module) to the electric field (Equation (3)).

$$\varepsilon = V_1\varepsilon_1 + V_2\varepsilon_2 \qquad \textbf{(2)}$$

$$1/\varepsilon = V_1/\varepsilon_1 + V_2/\varepsilon_2 \qquad \textbf{(3)}$$

Where ε_1 and ε_2 are the permittivity of phase 1 and phase 2, respectively; V_1 and V_2 ($V_1 + V_2 = 1$) are the volume fractions of these two phases. Here, the LM/LBMV heterogeneous multilayer ceramics can be treated with a series module, and the permittivity thereof were calculated, as shown in **Figure 5b** and **Table S1**. It is found that the measured permittivity data of LM/LBMV heterostructures are in accordance with the predicted ones by the series module, indicating that the dielectric properties of LM and LBMV are uncompromised after co-firing.

Figure 5c summarizes the microwave dielectric properties of recently developed co-fired heterogeneous dielectric materials. Compared with the previous studies, the LM/LBMV heterogeneous multilayer ceramics derived from self-constrained sintering are gifted with the virtues of much lower sintering temperature (~600 °C), free of glass phase, and hence superior comprehensive microwave dielectric properties.

4. Conclusions.

In summary, heterogeneous multilayer ceramics based on two representative microwave dielectric materials, low-K Li_2MoO_4 (LM) and high-K $[(Li_{0.5}Bi_{0.5})_xBi_{1-x}][Mo_xV_{1-x}]O_4$($x=0.098$) (LBMV) were prepared by the self-constrained sintering technique at an ultralow temperature of 600 °C. The high-K non-shrinking LBMV with a higher sintering temperature acts as a constrained layer to the low-K LM with a lower sintering temperature when densifying at low temperatures, and their roles reverse at high temperatures, yielding significantly suppressed in-plane shrinkage in the LM/LBMV heterogeneous multilayer ceramics. Moreover, the heterostructures are endowed with decent mechanical and microwave dielectric properties, demonstrating the great potential of self-constrained sintering for ULTCC applications.

Conflict of Interest

The authors declare no conflict of interest.

Acknowledgements

The work was supported by the National Key Research Program (Grant No. 2017YFB0406303).

References

1 Sebastian MT. *Dielectric materials for wireless communication*. London, UK: Elsevier, 2008.

2 Imanaka Y. *Multilayered Low Temperature Cofired Ceramics (LTCC) Technology*. Boston, USA: Springer-Verlag, 2004.

3 Reaney IM, Iddles D. Microwave Dielectric Ceramics for Resonators and Filters in Mobile Phone Networks. J Am Ceram Soc. 2006; 89: 2063-2072.

4 Sebastian MT, Wang H, Jantunen H. Low temperature co-fired ceramics with ultra-low sintering temperature: A review. Curr Opin Solid State Mater. 2016; 20: 151-170.

5 Liu B, Liu XQ, Chen XM. $Sr_2LaAlTiO_7$: a new Ruddlesden–Popper compound with excellent microwave dielectric properties. J Mater Chem C. 2016; 4: 1720-1726.

6 Lei SH, Fan HQ, Ren XH, Fang JW, Ma LT, Liu ZY. Novel sintering and band gap engineering of $ZnTiO_3$ ceramics with excellent microwave dielectric properties. J Mater Chem C. 2017; 5: 4040-4047.

7 Xia WS, Li LX, Ning PF, Liao QW. Relationship Between Bond Ionicity, Lattice Energy, and Microwave Dielectric Properties of $Zn(Ta_{1-x}Nb_X)_2O_6$ Ceramics. J Am Ceram Soc. 2012; 95: 2587-2592.

8 Zhang J, Luo Y, Yue ZX, Li LT. High-Q and temperature-stable microwave dielectrics in layer cofired $Zn_{1.01}Nb_2O_6/TiO_2/Zn_{1.01}Nb_2O_6$ ceramic architectures. J Am Ceram Soc. 2019; 102: 342-350.

9 Xiang HC, Bai Y, Varghese J, Li CC, Fang L, Jantunen H. Ultralow temperature cofired $BiZn_2VO_6$ dielectric ceramics doped with B_2O_3 and Li_2CO_3 for ULTCC applications. J Am Ceram Soc. 2019; 102: 1218-1226.

10 Mirsaneh M, Leisten OP, Zalinska B, Reaney IM. Circularly Polarized Dielectric-Loaded

Antennas: Current Technology and Future Challenges. Adv Funct Mater. 2008; 18: 2293-2300.

11 Ma M, Khan H, Shan W, Wang Y, Ou JZ, Liu Z, Kourosh KZ, Li Y. A novel wireless gas sensor based on LTCC technology. Sensors and Actuators B: Chemical. 2017; 239: 711-717.

12 Lei W, Zou ZY, Chen ZH, Ullah B, Zeb A, Lan XK, Lu WZ, Fan GF, Wang XH, Wang XC. Controllable τ_f value of barium silicate microwave dielectric ceramics with different Ba/Si ratios. J Am Ceram Soc. 2018; 101: 25-30.

13 Lim WB, Cho YS, Seo YJ, Park JG. Shrinkage behavior of LTCC hetero-laminates. J Eur Ceram Soc. 2009; 29:711-716.

14 Choi YJ, Park JH, Park JH, Nahm S, Park JG. Middle-and high-permittivity dielectric compositions for low-temperature co-fired ceramics. J Eur Ceram Soc. 2007; 27: 2017-2024.

15 Yang HC, Zhang SR, Yang HY, Yuan Y, Li EZ. Influence of $(Al_{1/3}W_{2/3})^{5+}$ co-substitution for Nb^{5+} in $NdNbO_4$ and the impact on the crystal structure and microwave dielectric properties. Dalton Trans. 2018; 47: 15808-15815.

16 Choi YJ, Park JH, Ko WJ, Hwang IS, Park JH, Park JG. Co-Firing and Shrinkage Matching in Low-and Middle-Permittivity Dielectric Compositions for a Low-Temperature Co-Fired Ceramics System. J Am Ceram Soc. 2006; 89: 562-567.

17 Ko WJ, Choi YJ, Park JH, Nahm S, Park JG. Co-Firing of Low-and High Permittivity Dielectric Tapes for Multifunctional Low-Temperature Co-Fired Ceramics. Ferroelectrics. 2006; 333: 193-202.

18 Sakamoto S, Adachi H, Kaneko K, Sugimoto Y, Takada T. Novel Low Temperature Co-Fired Ceramic Material System Composed of Dielectrics with Different Dielectric Constants. Jpn J Appl Phys. 2013; 52: 09KH03.

19 Murata T, Ohga S, Sugimoto Y. Development of a Novel Low Temperature Co-Fired Ceramics System Composed of Two Different Co-Firable Low Temperature Co-Fired Ceramics Materials. Jpn J Appl Phys. 2006; 45: 7401-7404.

20 Kim JS, Rudkin RA, Wang X, Atkinson A. Constrained sintering kinetics of 3YSZ films. J Eur Ceram Soc. 2011; 31: 2231-2239.

21 Mohanram A, Lee SH, Messing GL, Green DJ. Constrained Sintering of Low-Temperature Co-Fired Ceramics. J Am Ceram Soc. 2006; 89: 1923-1929.

22 Lee CF, Wu CF, Jean JH. Effects of CuO on constrained sintering of a polycrystalline TiO_2 ceramics. J Am Ceram Soc. 2019; 102: 158-166.

23 Qiu MH, Feng J, Fan YQ, Xu NP. Pore evolution model of ceramic membrane during constrained sintering. J Mater Sci. 2009; 44: 689-699.

24 Guo HZ, Guo J, Baker A, Randall CA. Hydrothermal-Assisted Cold Sintering Process: A New Guidance for Low Temperature Ceramic Sintering. ACS Appl Mater Interfaces. 2016; 8(49):34170-34170.

25 Wang DW, Zhou D, Song K, Feteira A, Randall CA, Reaney IM. Cold-Sintered C0G Multilayer Ceramic Capacitors. Adv Electron Mater. 2019; 1900025.

26 Guo J, Baker AL, Guo H, Lanagan M, Randall CA. Cold sintering process: A new era for ceramic packaging and microwave device development. J Am Ceram Soc. 2017; 100: 669-677.

27 Guo J, Pfeiffenberger N, Beese A, et al. Cold Sintering $Na_2Mo_2O_7$ Ceramic with Poly(ether imide) (PEI) Polymer to Realize High-Performance Composites and Integrated Multilayer Circuits. ACS Appl Nano Mater. 2018; 1: 3837-3844.

28 Funahashi S, Guo H, Guo J, et al. Cold sintering and co-firing of a multilayer device with thermoelectric materials J Am Ceram Soc. 2017; 00: 1-9.

29 Berbano SS, Guo J, Guo H, Lanagan MT, Randall CA. Cold sintering process of $Li_{1.5}Al_{0.5}Ge_{1.5}(PO_4)_3$ solid electrolyte. J Am Ceram Soc. 2017; 00: 1-13.

30 Liao CH, Jean JH, Hung YY. Self-Constrained Sintering of a Multilayer Low-Temperature-Cofired Glass-Ceramics/Alumina Laminate. J Am Ceram Soc. 2008; 91: 648-651.

31 You JH, Yeo DH, Shin HS, Kim JH, Yoon HG. Self-constrained sintering of Al_2O_3/glass/Al_2O_3 ceramics by glass infiltration. J Electroceram. 2009; 23: 367-371.

32 Chang JC, Jean JH. Self-Constrained Sintering of Mixed Low-Temperature-Cofired Ceramic Laminate. J Am Ceram Soc. 2006; 89: 829-835.

33 Rabe T, Schiller WA, Hochheimer T, Modes C, Kipka A. Zero Shrinkage of LTCC by Self-Constrained Sintering. Int J Appl Ceram Technol. 2005; 2: 374-382.

34 Zhou D, Randall CA, Wang H, Pang LX, Yao X. Microwave Dielectric Ceramics in Li_2O-Bi_2O_3-MoO_3 System with Ultra-Low Sintering Temperatures. J Am Ceram Soc. 2010; 93: 1096-1100.

35 Zhou D, Randall CA, Wang H, Pang LX, Yao X. Ultra-Low Firing High-k Scheelite Structures Based on $[(Li_{0.5}Bi_{0.5})_xBi_{1-x}][Mo_xV_{1-x}]O_4$ Microwave Dielectric Ceramics. J Am Ceram Soc. 2010; 93: 2147-2150.

36 Zhou D, Pang LX, Wang DW, Reaney IM. $BiVO_4$ based high k microwave dielectric materials: a review. J Mater Chem C. 2018; 6: 9290-9313.

Figure and Table Caption List:

Figure 1. Schematic drawing of the fabrication process of the LM/LBMV heterogeneous multilayer ceramics.

Figure 2 (a) XRD patterns of $BiVO_4$, LBMV and LM ceramics; the enlarged **(b)** (001) and **(c)** (020) peaks of $BiVO_4$ and LBMV ceramics. **(d)** Sintering temperature dependence of average grain size of LM and LBMV ceramics. **(e)** Evolution of microstructure of LM/LBMV multilayer ceramics with sintering temperature from 500 °C to 600 °C.

Figure 3 (a) Photograph of the LM/LBMV multilayer ceramics. **(b-d)** Cross-section SEM images of the LM/LBMV multilayer ceramics with different scales. EDX elemental maps of **(f)** Mo, **(g)** Bi, **(i)** V, and **(j)** O for the LM/LBMV multilayer ceramics highlighted by a yellow square in figure **(e)**; **(h)** EDX line scan across the LM/LBMV interfaces.

Figure 4 (a) Hardness of LM, LBMV and LM/LBMV heterogeneous multilayer samples. Sintering temperature dependence of shrinkage along the in-plane and out-plane directions of **(b)** pure LM and LBMV samples, and **(c)** LM/LBMV multilayer ceramics. **(d)** Shrinkage ratio out-plane/in-plane of LM, LBMV and LM/LBMV multilayer ceramics.

Figure 5 (a) Microwave dielectric properties of LM, LBMV ceramics and LM/LBMV multilayer ceramics sintered at 600 °C. **(b)** The measured and calculated permittivity of LM/LBMV multilayer ceramics as a function of sintering temperature. **(c)** Comparison of microwave dielectric properties of LM/LBMV multilayer ceramics with other co-firing hybrid dielectric materials.[16, 17, 18, 19]

Table 1. Sintering and dielectric properties of the materials of choice

		Sintering Properties	Dielectric Properties			
Abbreviation	Material	Optimal Sintering temp[°C]	Permittivity(ε_r)	Q × f [GHz]	TCF(τ_f) [ppm/°C]	Reference
LM	Li_2MoO_4	540	5.5	46000	-160	Ref. 28
LBMV	$[(Li_{0.5}Bi_{0.5})_xBi_{1-x}][Mo_xV_{1-x}]O_4$ x=0.098	650	81	8000	+10	Ref. 29

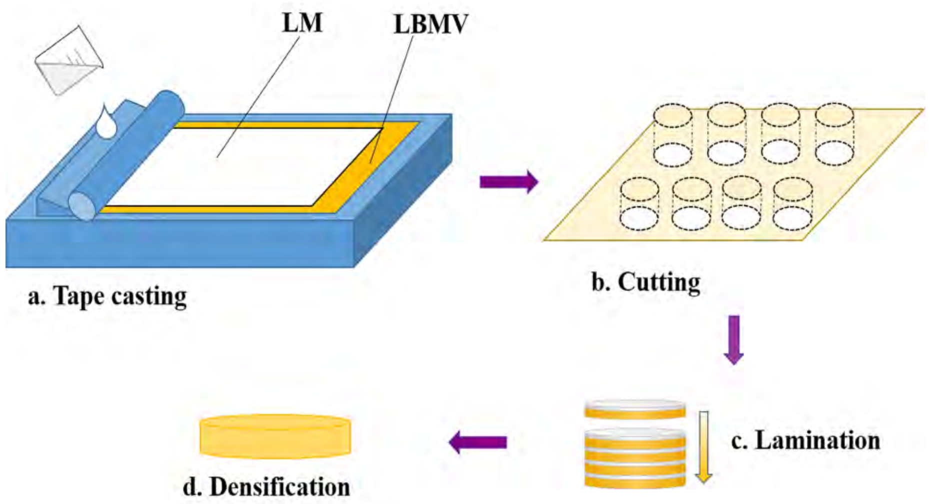
LM
LBMV
a. Tape casting
b. Cutting
c. Lamination
d. Densification

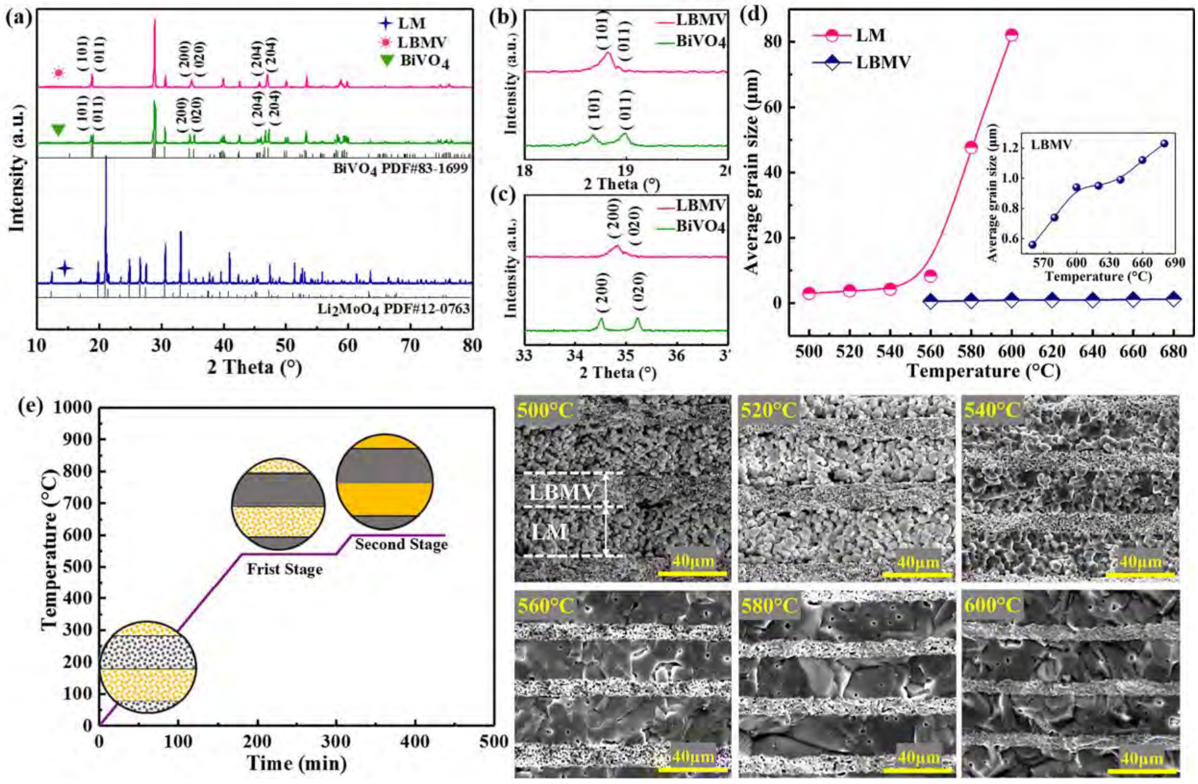
(a)
LM
LBMV
BiVO$_4$
(101)
(011)
(200)
(020)
(204)
(204)
BiVO$_4$ PDF#83-1699
Li$_2$MoO$_4$ PDF#12-0763
Intensity (a.u.)
2 Theta (°)
10
20
30
40
50
60
70
80
(b)
LBMV
BiVO4
Intensity (a.u.)
(101)
(011)
18
19
2 Theta (°)
(c)
LBMV
BiVO4
Intensity (a.u.)
(200)
(020)
33
34
35
36
2 Theta (°)
(d)
LM
LBMV
Average grain size (μm)
Temperature (°C)
0
20
40
60
80
500
520
540
560
580
600
620
640
660
680
LBMV
Average grain size (μm)
0.6
0.8
1.0
1.2
570
600
630
660
690
Temperature (°C)
(e)
Temperature (°C)
Time (min)
0
100
200
300
400
500
600
700
800
900
1000
Frist Stage
Second Stage
500°C
520°C
540°C
560°C
580°C
600°C
LBMV
LM
40μm

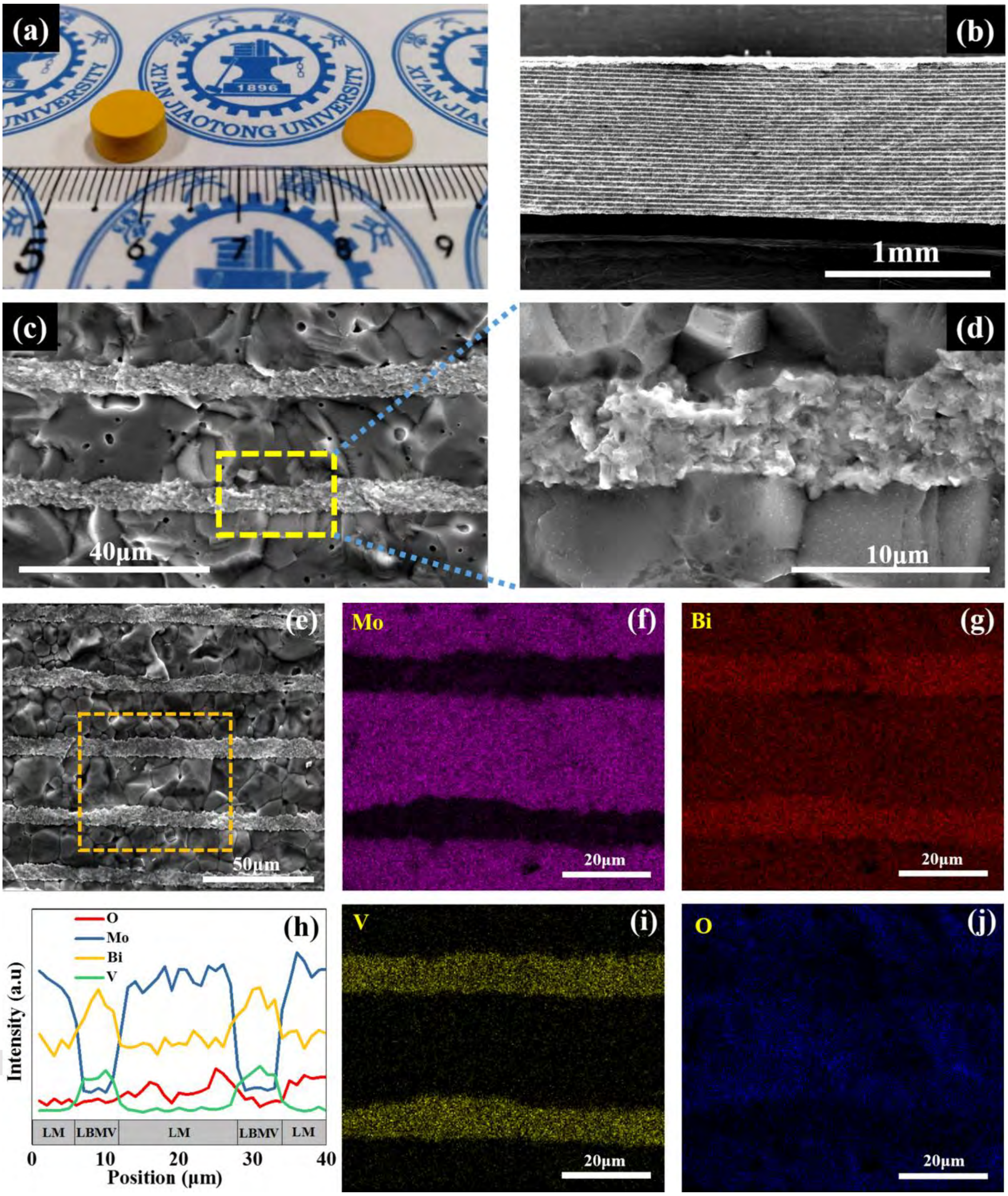
(a)
XI'AN JIAOTONG UNIVERSITY
1896
5
6
7
8
9
(b)
1mm
(c)
40μm
(d)
10μm
(e)
50μm
(f)
Mo
20μm
(g)
Bi
20μm
(h)
O
Mo
Bi
V
Intensity (a.u)
LM
LBMV
LM
LBMV
LM
0
10
20
30
40
Position (μm)
(i)
V
20μm
(j)
O
20μm

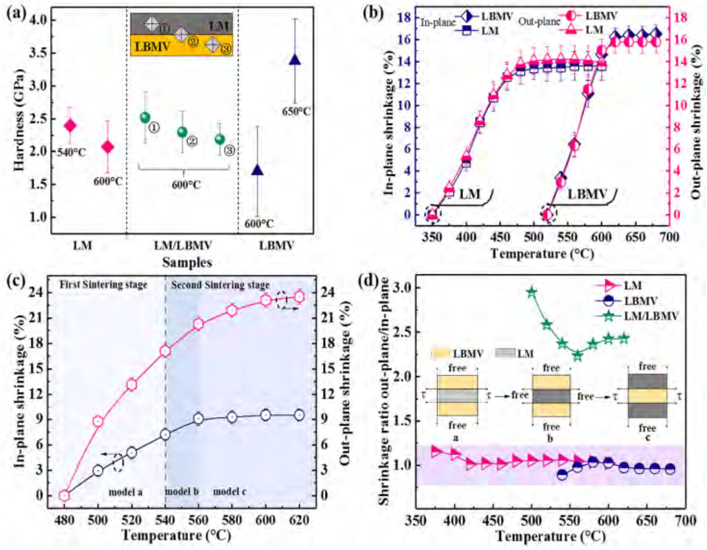
(a)
Hardness (GPa)
LM
LBMV
①
②
③
540°C
600°C
600°C
600°C
650°C
LM
LM/LBMV
LBMV
Samples
(b)
In-plane
LBMV
LM
Out-plane
LBMV
LM
In-plane shrinkage (%)
Out-plane shrinkage (%)
LM
LBMV
Temperature (°C)
(c)
First Sintering stage
Second Sintering stage
In-plane shrinkage (%)
Out-plane shrinkage (%)
model a
model b
model c
Temperature (°C)
(d)
LM
LBMV
LM/LBMV
LBMV
LM
free
τ
a
b
c
Shrinkage ratio out-plane/in-plane
Temperature (°C)

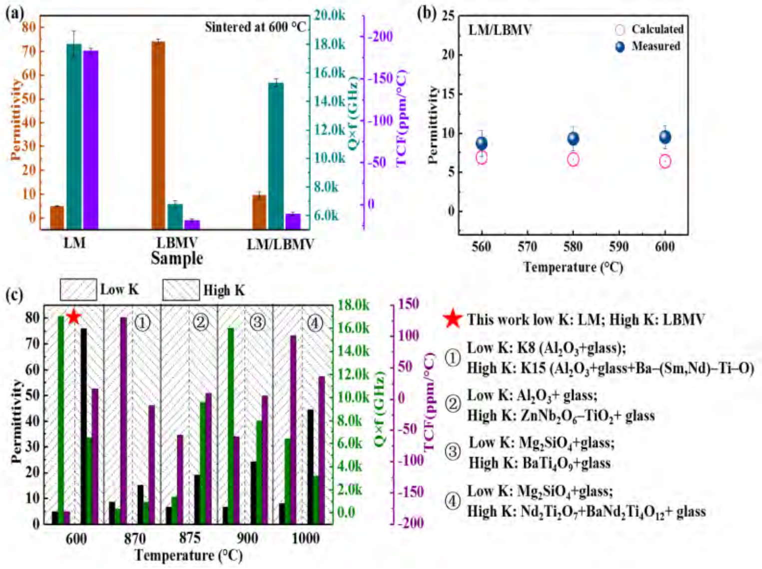
(a)
Sintered at 600 °C
Permittivity
Q×f (GHz)
TCF(ppm/°C)
LM
LBMV
LM/LBMV
Sample
(b)
LM/LBMV
Calculated
Measured
Permittivity
Temperature (°C)
(c)
Low K
High K
Permittivity
Q×f (GHz)
TCF(ppm/°C)
①
②
③
④
600
870
875
900
1000
Temperature (°C)
This work low K: LM; High K: LBMV
① Low K: K8 (Al2O3+glass); High K: K15 (Al2O3+glass+Ba–(Sm,Nd)–Ti–O)
② Low K: Al2O3+ glass; High K: ZnNb2O6–TiO2+ glass
③ Low K: Mg2SiO4+glass; High K: BaTi4O9+glass
④ Low K: Mg2SiO4+glass; High K: Nd2Ti2O7+BaNd2Ti4O12+ glass